

Design, Synthesis, Biochemical, and Antiviral Evaluations of C6 Benzyl and C6 Biarylmethyl Substituted 2-Hydroxyisoquinoline-1,3-diones: Dual Inhibition against HIV Reverse Transcriptase-Associated RNase H and Polymerase with Antiviral Activities

Sanjeev Kumar V. Vernekar,[†] Zheng Liu,^{†,||} Eva Nagy,[‡] Lena Miller,[‡] Karen A. Kirby,[§] Daniel J. Wilson,[†] Jayakanth Kankanala,[†] Stefan G. Sarafianos,[§] Michael A. Parniak,[‡] and Zhengqiang Wang^{*,†}

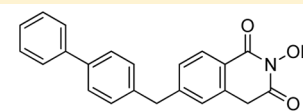
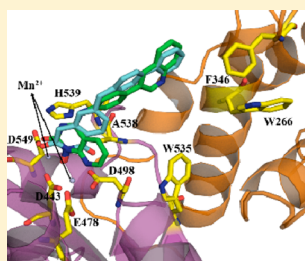
[†]Center for Drug Design, Academic Health Center, University of Minnesota, 516 Delaware Street SE, PWB 7-224, MMC 204 Minneapolis, Minnesota 55455, United States

[‡]Department of Microbiology & Molecular Genetics, University of Pittsburgh School of Medicine, 450 Technology Drive, Pittsburgh, Pennsylvania 15219, United States

[§]Department of Molecular Microbiology and Immunology and Department of Biochemistry, University of Missouri School of Medicine, Christopher S. Bond Life Sciences Center, Columbia, Missouri 65211, United States

S Supporting Information

ABSTRACT: Reverse transcriptase (RT) associated ribonuclease H (RNase H) remains the only virally encoded enzymatic function not targeted by current chemotherapy against human immunodeficiency virus (HIV). Although numerous chemotypes have been reported to inhibit HIV RNase H biochemically, few show significant antiviral activity against HIV. We report herein the design, synthesis, and biological evaluations of a novel variant of 2-hydroxyisoquinoline-1,3-dione (HID) scaffold featuring a crucial C-6 benzyl or biarylmethyl moiety. The synthesis involved a recently reported metal-free direct benzylation between tosylhydrazone and boronic acid, which allowed the generation of structural diversity for the hydrophobic aromatic region. Biochemical studies showed that the C-6 benzyl and biarylmethyl HID analogues, previously unknown chemotypes, consistently inhibited HIV RT-associated RNase H and polymerase with IC_{50} s in low to submicromolar range. The observed dual inhibitory activity remained uncompromised against RT mutants resistant to non-nucleoside RT inhibitors (NNRTIs), suggesting the involvement of binding site(s) other than the NNRTI binding pocket. Intriguingly, these same compounds inhibited the polymerase, but not the RNase H function of Moloney Murine Leukemia Virus (MoMLV) RT and also inhibited *Escherichia coli* RNase H. Additional biochemical testing revealed a substantially reduced level of inhibition against HIV integrase. Molecular docking corroborates favorable binding of these analogues to the active site of HIV RNase H. Finally, a number of these analogues also demonstrated antiviral activity at low micromolar concentrations.



20i
 IC_{50} (RNase H) = 0.8 μ M
 IC_{50} (Pol) = 1.6 μ M
 IC_{50} (IN) > 100 μ M
 EC_{50} (HIV-1) = 3.0 μ M
 CC_{50} = 50 μ M

INTRODUCTION

HIV infects an estimated 35 million people worldwide.¹ With the lack of effective vaccines^{2,3} and challenges in achieving viral eradication,⁴⁻⁶ managing HIV infection continues to rely heavily on antivirals for prophylaxis and therapy. Anti-HIV drugs targeting all three virally encoded enzymes: RT, integrase (IN), and protease, as well as viral entry proteins and cellular coreceptors, provide a large repertoire for the highly active antiretroviral therapy (HAART). Although largely efficacious, these regimens can be plagued by the emergence of resistant HIV mutants. Therefore, less explored and unvalidated viral targets key to HIV replication have become increasingly attractive for developing antivirals with novel mechanism of action to inhibit resistant viral strains. One such target is the RT associated RNase H activity.^{7,8} RT has two domains with distinct enzymatic functions essential for HIV replication:⁸ a polymerase

domain that carries out both RNA dependent DNA polymerization and DNA dependent DNA polymerization, and an RNase H domain that selectively degrades RNA from the RNA/DNA heteroduplex intermediate during reverse transcription. Current FDA-approved nucleoside RT inhibitors (NRTIs)⁹ and non-nucleoside RT inhibitors (NNRTIs)¹⁰ all target the DNA polymerase function of RT; inhibitors of RT-associated RNase H have yet to make it to the development pipeline.

The critical role of RNase H in HIV replication has long been recognized and efforts in targeting RNase H for antiviral development have identified a few active site inhibitor chemotypes (Figure 1),^{11,12} including HID (1),¹³ β -thujaplicinol (2),¹⁴ furan-2-carboxylic acid carbamoylmethyl ester (3),¹⁵ diketooacid

Received: July 28, 2014

Published: December 18, 2014

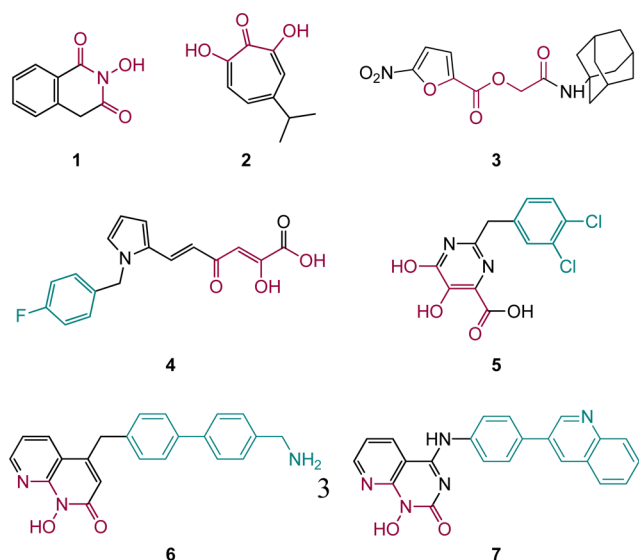


Figure 1. Major chemotypes reported as HIV RNase H active site inhibitors. Chemotypes 4–7 reflect a pharmacophore model consisting of a chelating triad (magenta) and an aryl or biaryl moiety (cyan) connected through a methylene or amino linker.

(4),¹⁶ the Gilead pyrimidinol carboxylic acid (5),¹⁷ the Merck naphthyridinone (6),¹⁸ and the GSK pyridopyrimidinone (7).^{19,20} These chemotypes all have a chelating triad (magenta) for competitive binding to the active site divalent metals. Structurally more elaborate chemotypes (4–7) also feature a hydrophobic aromatic moiety, typically an aryl (4–5) or biaryl (6–7), connected to the chelating core through a methylene or amino linker, conferring potent and selective RNase H inhibition. The biaryl substituent proved to be particularly effective as compounds 6–7 are among the very few RNase H inhibitors that demonstrate potent antiviral activity.^{18,19}

We are particularly interested in the HID chelating core because we have previously constructed C6/C7 aryl-substituted HID scaffolds for inhibiting hepatitis C virus NSSB.²¹ Other variants of HID have also been explored as HIV IN inhibitors.^{22–25} Klumpp et al. first reported the ability of HID (1) to inhibit HIV, but not the *Escherichia coli* RNase H,¹³ albeit without antiviral activity in cell-based assays (Figure 2). Improved inhibitory profile, including anti-HIV activity, was achieved by Billamboz et al. through C4 carboxylate substitution (Figure 2, compound 8).²⁶ As aforementioned, the best RNase H inhibitors known reflect a pharmacophore model that features a biaryl moiety. This pharmacophore model

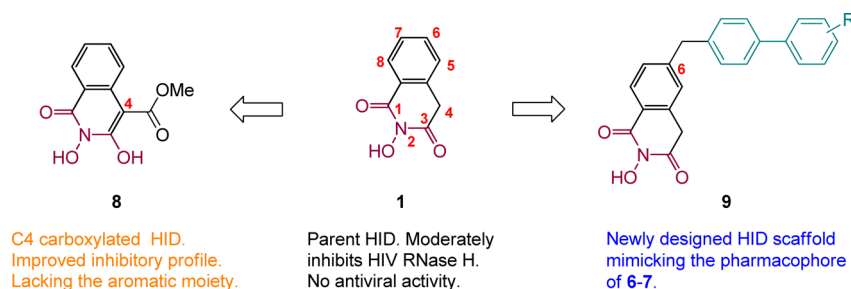
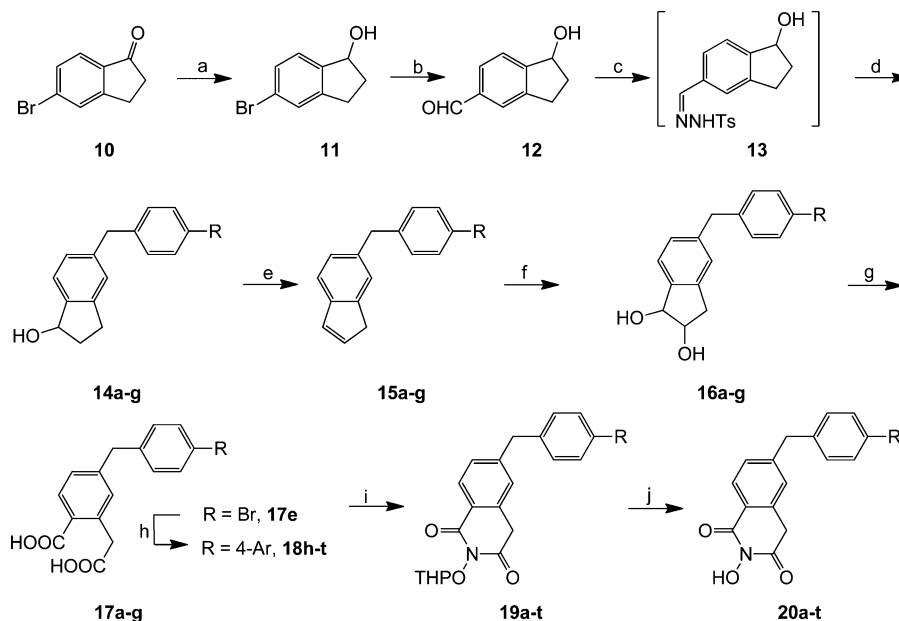


Figure 2. Design of a novel HID scaffold 9 based on the pharmacophore model of 4–7.

Scheme 1. Synthesis of C6 Arylmethyl HID Analogues 20a–t^a

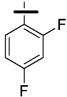
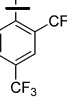
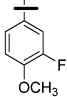
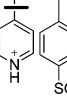


^aReagents and conditions: (a) NaBH₄, THF, rt, 12 h, 87%; (b) *n*-BuLi, DMF, THF, –78 °C–rt, overnight, 76%; (c) TsNHNH₂, toluene, 80 °C, 2 h; (d) boronic acid, K₂CO₃, 1,4-dioxane, 110 °C, 3–5 h, 40–55%; (e) PPTS, toluene, reflux, 6–12 h, 75–90%; (f) OsO₄, NMO, *t*-BuOH/acetone/H₂O, rt, 2–6 h, 60–81%; (g) NaIO₄, RuCl₃, CH₃CN/CCl₄/H₂O, rt, 2–4 h, 67–85%; (h) ArB(OH)₂, Pd(PPh₃)₄, K₂CO₃, EtOH/H₂O, microwave, 120–150 °C, 20–30 min, 60–75%; (i) NH₂OTHP, CDI, toluene, reflux, 12 h; (j) *p*-TSA hydrate, MeOH, 2–3 h, rt, 35–55% over two steps.

Table 1. Biochemical Inhibitory Activity of Compounds 20a–t against HIV RT RNase H and Polymerase

Cpd	R	Full-Length RT RNase H IC ₅₀ ^a (μM)			RNase H Fragment ^e IC ₅₀ (μM)	RT pol IC ₅₀ (μM)
		HTS-1 ^b	HTS-2 ^c	HTS-3 ^d		
20a	H	1.3 ± 0.1	1.4 ± 0.1	1.1 ± 0.05	1.1 ± 0.05	1.7 ± 0.3
20b	4-CH ₃	1.2 ± 0.1	1.3 ± 0.1	1.1 ± 0.2	0.9 ± 0.1	2.0 ± 0.3
20c	4-F	1.3 ± 0.1	0.80 ± 0.1	1.2 ± 0.1	0.5 ± 0.1	2.3 ± 0.7
20d	4-Cl	3.9 ± 0.2	3.7 ± 0.3	4.0 ± 0.15	2.9 ± 0.1	3.8 ± 0.3
20e	4-Br	1.4 ± 0.2	1.3 ± 0.2	1.1 ± 0.1	1.0 ± 0.1	1.5 ± 0.1
20f	4-CF ₃	1.5 ± 0.1	1.1 ± 0.3	2.0 ± 0.2	1.2 ± 0.1	3.3 ± 1.3
20g	2,4-F	1.6 ± 0.3	1.5 ± 0.05	1.0 ± 0.1	1.2 ± 0.2	2.3 ± 0.1
20h		0.60 ± 0.1	0.80 ± 0.05	0.90 ± 0.05	0.90 ± 0.05	1.3 ± 0.2
20i		0.80 ± 0.1	0.60 ± 0.1	0.90 ± 0.05	0.50 ± 0.15	1.6 ± 0.7
20j		2.7 ± 0.6	2.0 ± 0.3	2.7 ± 0.9	0.70 ± 0.2	1.5 ± 0.3
20k		5.4 ± 0.8	4.9 ± 1.1	5.0 ± 1.9	2.8 ± 0.2	3.7 ± 0.1
20l		0.90 ± 0.2	0.90 ± 0.2	0.90 ± 0.4	0.50 ± 0.2	0.75 ± 0.1
20m		3.0 ± 0.4	3.1 ± 0.3	2.0 ± 0.2	1.0 ± 0.1	2.5 ± 0.6
20n		1.2 ± 0.2	1.3 ± 0.5	1.4 ± 0.1	1.2 ± 0.05	1.8 ± 0.7
20o		0.40 ± 0.1	0.50 ± 0.2	0.50 ± 0.1	0.40 ± 0.15	0.5 ± 0.1
20p		2.4 ± 0.2	2.1 ± 0.5	2.9 ± 0.4	1.5 ± 0.15	2.6 ± 0.2

Table 1. continued

Cpd	R	Full-Length RT RNase H IC ₅₀ ^a (μM)			RNase H Fragment ^e IC ₅₀ (μM)	RT pol IC ₅₀ (μM)
		HTS-1 ^b	HTS-2 ^c	HTS-3 ^d		
20q		1.5 ± 0.5	0.90 ± 0.15	1.4 ± 0.2	0.70 ± 0.05	2.0 ± 0.1
20r		5.1 ± 0.6	8.7 ± 0.9	5.6 ± 0.3	2.5 ± 0.3	6.5 ± 0.6
20s		2.2 ± 0.6	1.8 ± 0.3	1.2 ± 0.15	0.70 ± 0.05	1.9 ± 0.2
20t		0.50 ± 0.05	1.3 ± 0.15	1.0 ± 0.1	0.80 ± 0.1	0.9 ± 0.1
1	--	1.2 ± 0.1	1.0 ± 0.2	0.60 ± 0.05	0.50 ± 0.2	>25

^aIC₅₀: concentration of a compound producing 50% inhibition, expressed as mean ± standard deviation from at least three independent experiments. ^bSubstrate that measures internal cleavage. ^cSubstrate that measures DNA 3' end directed cleavage. ^dSubstrate that measures RNA 5' end directed cleavage. ^eReconstituted HIV RNase H domain.

prompted us to design a previously unknown variant of HID (Figure 2, chemotype 9). We report herein the chemical synthesis, biochemical and antiviral evaluations, and molecular modeling of 9.

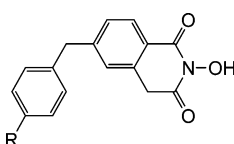
RESULTS AND DISCUSSION

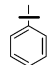
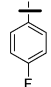
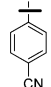
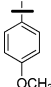
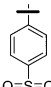
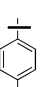
Chemistry. The synthetic chemistry for constructing HID ring has been well established. The synthesis typically involves a Hurlley reaction for parent HID (1) or C4 carboxylated HID (8).^{26,27} A synthetic handle on C6/C7 position, particularly a halogen or amino group, also allowed variation of HID through similar synthetic routes.^{21,27} This general strategy, however, proved unsuccessful toward the synthesis of our newly designed HID chemotype 9. The C6 benzylation in this case turned out to be a major synthetic hurdle. After several unsuccessful attempts, we were able to work out a synthetic route that allowed the synthesis of a library of 20 6-benzyl or biarylmethyl substituted 2-hydroxyisoquinoline-1,3(2*H*,4*H*)-dione analogues in 9–10 steps (Scheme 1). Key to this approach was the adaptation of a one-pot benzylation procedure²⁸ for the formation of C–C bond reported by Valdés and co-workers, which involves a reductive coupling of aldehyde 12 with a boronic acid in the presence of a base (steps c–d, Scheme 1). The employment of various boronic acids in this step generated the structural diversity for the C6 benzyl series of analogues. Another prominent feature of this synthesis is the masking of the requisite dicarboxylic acid (17) with an alcohol handle (12) to facilitate the key benzylation. The diversity for the second series, the C6 biarylmethyl HID, was introduced much later in the synthesis (step h, Scheme 1) via Suzuki coupling.

The detailed synthesis is depicted in Scheme 1. To begin the synthesis, commercially available 5-bromoindan-1-one (10)

was reduced to alcohol 11 with NaBH₄, followed by a direct formylation with *N,N*-dimethylformamide (DMF) and *n*-BuLi to afford aldehyde 12 in good yield. The subsequent benzylation was carried out via a two-step sequence: the formation of tosylhydrazone 13 by treating aldehyde 12 with tosylhydrazine, and the reductive coupling of 13 with various boronic acids to produce 5-arylmethylindanones (14a–g).²⁸ Although this two-step benzylation process worked with only moderate yields, it did tolerate a range of functional groups. The elaboration from alcohols 14a–g to diacids 17a–g was achieved in three steps: first, a dehydration by treating with pyridinium *p*-toluenesulfonate (PPTS) at reflux toluene furnished alkenes 15a–g in good to excellent yields, second, an Upjohn dihydroxylation^{29,30} of alkenes 15a–g yielded diols 16a–g under ambient temperature, and third, an oxidative cleavage of 1,2 diols 16a–g with NaIO₄ and RuCl₃³¹ resulted in intermediate homophthalic acid derivatives 17a–g in good yields. At this point, a series of C6 biarylmethyl diacids (18h–t) were obtained via Suzuki coupling from 4-Br intermediate diacid 17e. Finally, the target scaffold 9 as represented by analogues 20a–t was constructed by the condensation of diacids 17a–g and 18h–t with *O*-tetrahydropyran (THP) protected hydroxylamine in the presence of carbonyldiimidazole (CDI) in refluxing toluene. The isolation of cyclized products 19a–t from the reaction mixture proved to be rather straightforward by flash column chromatography. This cyclization followed by the deprotection of THP under *p*-toluenesulfonic acid (*p*-TSA) afforded target compounds 20a–t in 35–55% yield over two steps.

Biology. All newly synthesized analogues were evaluated biochemically for inhibition in RNase H and/or polymerase assays of HIV RT, MoMLV RT, and *E. coli* RNase H, as well as in an HIV IN strand transfer assay. Antiviral activity was

Table 2. Biochemical Inhibitory Activity of Selected Compounds against RNase H and Polymerase Functions of NNRTI-Resistant HIV RT Mutants


Cpd	R	Y181C mutant IC ₅₀ ^a (μM)			L100I/K103N mutant IC ₅₀ ^a (μM)		
		RNase H HTS-1 ^b	RNase H HTS-2 ^b	pol	RNase H HTS-1 ^b	RNase H HTS-2 ^b	pol
20d	4-Cl	7.0 ± 0.9	9.0 ± 0.3	5.3 ± 1.0	8.2 ± 0.3	8.7 ± 2.5	5.1 ± 0.4
20i		0.9 ± 0.5	1.1 ± 0.6	0.7 ± 0.2	0.7 ± 0.1	1.0 ± 0.4	0.5 ± 0.1
20k		4.7 ± 3.4	7.2 ± 4.8	1.7 ± 0.1	2.5 ± 0.2	2.5 ± 0.6	1.5 ± 0.1
20l		1.3 ± 0.8	1.8 ± 1.3	0.8 ± 0.3	0.9 ± 0.2	0.8 ± 0.2	0.3 ± 0.1
20m		3.8 ± 0.5	3.9 ± 1.0	1.7 ± 0.3	1.3 ± 0.3	1.9 ± 0.1	1.0 ± 0.1
20n		0.8 ± 0.1	1.4 ± 0.4	0.7 ± 0.2	1.2 ± 0.1	1.4 ± 0.1	0.5 ± 0.1
20o		0.2 ± 0.05	0.3 ± 0.1	0.3 ± 0.1	0.4 ± 0.05	0.3 ± 0.1	0.2 ± 0.05

^aIC₅₀: concentration of a compound producing 50% inhibition, expressed as mean ± standard deviation from at least three independent experiments.

^bRNase H substrates as described in the Experimental Section.

assessed in cell-based assays and antiviral EC₅₀ and cytotoxicity CC₅₀ values were generated for selected analogues.

All New C6 Benzyl and C6 Biarylmethyl HID Analogues Potently Inhibit HIV RT Associated RNase H and Polymerase. RNA cleavage by RNase H is required at multiple stages of reverse transcription and could involve at least three distinct modes of RNase H cleavages:¹² the random internal cleavages which likely represent the majority of RNase H event during reverse transcription, the DNA 3' end directed and polymerase dependent cleavages which allow specific RNA cuts 17–18 nucleotides downstream from the polymerase active site, and the RNA 5' end directed cleavages which degrade the recessed RNA template. The RNase H inhibitory activity of our compounds was assessed using three different oligonucleotide duplexes as described in the Experimental Section. Substrate HTS-1 is a short (18 bp) duplex that measures internal cleavages and is highly sensitive to inhibitors,^{32–34} substrate HTS-2 assesses DNA 3' end directed cleavages, and substrate HTS-3 evaluates RNA 5' end directed cleavages. Detailed assay results are summarized in Table 1. Overall, our newly synthesized HID analogues, both the C6 benzyl series (**20a–h**) and C6 biarylmethyl series

(**20i–t**), potently inhibited all three forms of RNase H cleavage with virtually equal potencies. Interestingly, while almost all compounds within the C6 benzyl series (**20a–g**) were active in low micromolar range, quite a few analogues of the C6 biarylmethyl series (**20i**, **20l**, **20o**, **20r**, and **20t**) demonstrated submicromolar activities, suggesting that the additional aromatic ring can be advantageous for the biochemical inhibitory activity. Another key observation was the relatively flat structure–activity relationship (SAR) around the C6 benzyl series where all analogues exhibited a similar IC₅₀ value (1.2–1.6 μM) except for the 4-cyclopropyl derivative (**20h**, IC₅₀ = 0.6 μM) and the 4-Cl analogue (**20d**, IC₅₀ = 3.9 μM). By contrast, the C6 biarylmethyl series showed greater variation in IC₅₀ values with two notable SAR trends: (1) a fluoro group on the terminal aromatic ring did not enhance biochemical inhibition (**20k** and **20q** vs **20i**), which represents a significant departure from the canonical IN inhibitor pharmacophore model where such a fluoro group typically benefit target binding substantially; (2) a strong electron-withdrawing group with H-bonding ability, such as cyano (**20l**) sulfonamide (**20o**), and pyridine (**20t**), appeared to confer the most potent biochemical

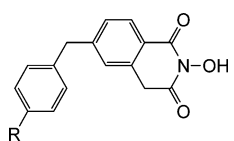
inhibition. These observations corroborate an inhibitor binding mode where the terminal aromatic group makes critical contacts with the RNA/DNA substrate. Further biochemical evaluation with a reconstituted and catalytically active RNase H domain confirmed the observed potency and SAR trends (Table 1, RNase H fragment).


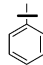
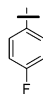
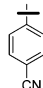
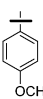
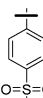
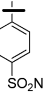
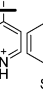
In parallel to the RNase H assays, all compounds were also tested in a classic RT polymerase assay with poly(A) as template, poly(dT) as primer and [³H]dTTP. The results are listed in Table 1. Interestingly, our compounds inhibited polymerase with potencies nearly equal to RNase H inhibition while a control compound (**1**) showed a selective profile toward RNase H inhibition consistent with previous report.¹³ Selected analogues were further tested against NNRTI-resistant HIV RT single (Y181C) and double (L100I/K103N) mutants. These assays yielded IC₅₀ values against both RNase H and polymerase largely in range with those of WT RT (Table 2), strongly suggesting that our compounds do not occupy the NNRTI pocket. Although the exact mechanism of polymerase inhibition is not clear, it is conceivable that, with the chelating triad, these compounds could compete for polymerase active site binding. It is also possible that they may bind at an unknown site of RT and affect both polymerase and RNase H activities. Nevertheless, previous work on similar HID scaffolds has reported selective inhibition against HIV RNase H,^{13,26} IN,²³ or dual inhibition against both.^{22,27} The unique and potent dual inhibition of our compounds against RT RNase H and polymerase will add to the activity profile of these important compounds and may contribute to achieving the elusive antiviral activity for RNase H-targeting HID compounds.

To further establish the biochemical inhibitory profile of our compounds, we also tested selected compounds against *E. coli* RNase H and MoMLV RT RNase H and polymerase activities. As shown in Table 3, all analogues demonstrated single-digit μM activity against *E. coli* RNase H. For MoMLV RT, no inhibitory activity was detected against RNase H and low μM activity was observed against polymerase (Table 3). These results suggest that dual inhibition of both RT functions can be achieved with HIV RT only.

Some C6 Benzyl and C6 Biarylmethyl HID Analogues Moderately Inhibit HIV IN. RNase H enzymes form a signature fold at the active site that defines a whole family of highly homologous enzymes termed as retroviral integrase superfamily (RISF).³⁵ Members of this family of enzymes, including HIV IN, adopt a very similar active site fold as RNase H. As a result, achieving selective RNase H inhibition over IN inhibition represents a major challenge in RNase H inhibitor discovery. To gauge the selectivity profile of our new HID chemotype, we tested all compounds in an HIV IN strand transfer (ST) assay. The results are summarized in Table 4. Notably, with the exception of **20f**, which did not show any activity at concentrations up to 100 μM, all compounds within the C6 benzyl HID series (**20a–h**) demonstrated significant activity against HIV IN at low micromolar concentrations with IC₅₀ values ranging between 3.8 and 36 μM. This observation conforms to the pharmacophore model of IN ST inhibitors where a chelating triad and a terminal benzyl group are the two major structural determinants.³⁶ Nevertheless, most compounds within this series inhibited IN with a considerably higher IC₅₀ than that for RNase H inhibition. Furthermore, the IN inhibitory activity was drastically reduced when a second aromatic ring was introduced to the benzyl terminus, resulting in the biarylmethyl HID series (**20i–t**). Seven out of the 12 analogues within this series

Table 3. Biochemical Inhibitory Activity of Selected Compounds against *E. coli* RNase H and MoMLV RT RNase H and Polymerase Activities

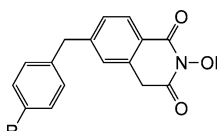


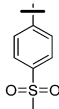
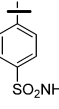
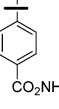
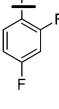
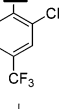
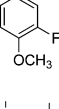
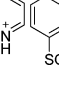

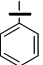
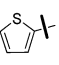
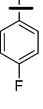
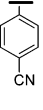
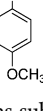
Compd	R	<i>E. coli</i>	MoMLV RT	MoMLV RT
		RNase H	RNase H	pol
		IC ₅₀ ^a (μM)	IC ₅₀ (μM)	IC ₅₀ (μM)
20a	H	6.5 ± 1.3	>30	3.2 ± 1.1
20d	4-Cl	4.5 ± 1.2	>30	7.1 ± 1.1
20f	4-CF ₃	7.2 ± 1.2	>30	6.9 ± 1.2
20h		3.2 ± 1.3	>30	3.1 ± 1.1
20i		3.4 ± 1.3	>30	13 ± 1.2
20k		2.9 ± 1.3	>30	11 ± 1.2
20l		3.2 ± 1.2	>30	8.5 ± 1.2
20m		3.1 ± 1.3	>30	11 ± 1.2
20n		7.2 ± 1.2	>30	3.9 ± 1.1
20o		2.5 ± 1.3	>30	2.4 ± 1.1
20t		4.0 ± 1.3	>30	2.8 ± 1.4

^aIC₅₀: concentration of a compound producing 50% inhibition, expressed as mean ± standard deviation from two independent experiments of duplicates.

showed no activity against IN at concentrations up to 100 μM, leading to excellent selectivity toward RNase H inhibition (Table 4, compounds **20i–m**, **20q**, and **20s**). Others (**20n–p**, **20r**, and **20t**) inhibited IN in low micromolar range, yet still with a sizable nominal selectivity (3.8–16-fold, Table 4) toward RNase H inhibition. Although intractable variables involved in biochemical assays render it unreliable to quantitatively correlate distinct biochemical assays (IN vs RNase H and pol), the general lack of IN inhibition and the potent anti-RNase H and antipolymerase activities of the biarylmethyl series could indicate that it is possible to develop RT dual inhibitors without inhibiting IN based on this particular chemotype.

Table 4. Biochemical Inhibitory Activity of Compounds 20a–t against HIV IN



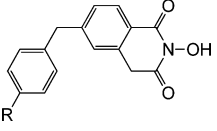
Compd	R	RNase H IC ₅₀ ^a (μM)	IN IC ₅₀ ^b (μM)	SI ^c	Compd	R	RNase H IC ₅₀ ^a (μM)	IN IC ₅₀ ^b (μM)	SI ^c
20a	H	1.3 ± 0.1	3.8 ± 0.7	2.9	20n		1.2 ± 0.2	11 ± 7.4	9.2
20b	4-CH ₃	1.2 ± 0.1	36 ± 15	30	20o		0.40 ± 0.1	3.6 ± 1.5	9.0
20c	4-F	1.3 ± 0.1	36 ± 25	28	20p		2.4 ± 0.2	9.1 ± 2.7	3.8
20d	4-Cl	3.9 ± 0.2	4.4 ± 0.5	1.1	20q		1.5 ± 0.5	>100	>67
20e	4-Br	1.4 ± 0.2	28 ± 6.4	20	20r		0.57 ± 0.22	9.1 ± 2.6	16
20f	4-CF ₃	1.5 ± 0.1	>100	>67	20s		2.2 ± 0.6	>100	>45
20g	2,4-F	1.6 ± 0.3	20 ± 5.5	13	20t		0.50 ± 0.05	5.7 ± 2.4	11
20h		0.60 ± 0.1	3.8 ± 1.6	6.3					
20i		0.80 ± 0.1	>100	>130					
20j		2.7 ± 0.6	>100	>37					
20k		5.4 ± 0.8	>100	>19					
20l		0.90 ± 0.2	>100	>110					
20m		3.0 ± 0.4	>100	>33					

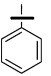
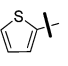
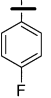
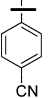
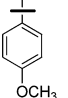
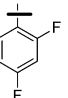
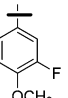
^aData with HTS-1 as substrate. ^bExpressed as mean ± standard deviation from at least three independent experiments. ^cSelectivity index defined by IC₅₀ IN/IC₅₀ RNase H.

Many C6 Benzyl and C6 Biarylmethyl HID Analogues Inhibit HIV-1 in Low Micromolar Range. To assess the ability of our new C6 benzyl and biarylmethyl HID chemotypes in inhibiting HIV replication in cell culture, we have carried out a single replication cycle antiviral assay.^{37,38} This assay quantitatively measures HIV infection in indicator cells (P4R5) through the expression of a Tat-dependent reporter (β -galactosidase) and quickly determines the infectivity/inhibition with only one replication cycle by colorimetric analysis after incubation with a β -galactosidase substrate. We tested all 20 newly synthesized HID analogues in this antiviral assay, and nine of them inhibited HIV replication in low micromolar range (Table 5), with compound 20i being the most potent with an antiviral EC₅₀ of 3.0 μM. Although compounds of a few chemotypes have been reported to biochemically inhibit HIV RNase H, a limited number demonstrated significant antiviral

activities, which signifies the challenge for small molecules to compete against much larger RNA/DNA substrates for active site binding. Achieving antiviral activity with RNase H active site inhibitors entails exceptionally tight binding only achieved with a few compounds.²⁰ The consistent and low micromolar antiviral activity observed with our compounds may reflect the benefits of additional polymerase inhibition in overcoming the biochemical barrier of competing against endogenous substrates.

RNase H Active Site Binding. To confirm the RNase H active site binding mode of our new chemotypes, we have conducted molecular modeling where a selected analogue 20i was docked along with the potent GSK-5724 (7) into the crystal structure of full length RT cocrystallized with naphthyridinone-based scaffold MK2 (PDB code: 3LP1).³⁹ The full length RT consists of two domains, the p66 subunit with fingers (blue), palm (red), thumb (green), connection (yellow), and RNase H (magenta)

Table 5. Antiviral Potency of Selected Analogues^a


Compd	R	Anti-HIV EC ₅₀ (μM)	CC ₅₀ (μM) ^b	TI
20c	4-F	13	> 50	> 4
20f	4-CF ₃	6.2	50	8
20i		3.0	50	17
20j		13	> 50	> 4
20k		10	n.d. ^c	--
20l		13	> 50	> 4
20m		10	n.d.	--
20q		13	> 50	> 4
20s		13	> 50	> 4

^aAll values are averages of two separate determinations. ^b50 μM was the highest concentration tested. ^cn.d., not determined.

subdomains, and the p51 subunit (orange) as shown in Figure 3, left. The above RT structure was subjected to analysis and found that the naphthyridinone was bound to the active site of RNase H, which is ~50 Å from the NNRTI site. The docking analysis was performed using Glide (Schrodinger Inc.).⁴⁰ The predicted binding modes of both the compounds within the active site of RNase H are shown in Figure 3, right.

The predicted binding mode of compound 7 within the active site of RNase H suggests a potential interaction between the pyridopyrimidinone core (chelating triad) and the two metal cofactors (Mn²⁺), which are coordinated to the active site acidic residues D443, E478, D498, and D549. The binding pocket is lined up with the residues G444, S449, A538, H539, W535, V552, and S553 of the p61 subunit and N265, W266, F346, and W535 of the p51 subunit. The biaryl moiety is extended into the small hydrophobic region of the RNase H, which could potentially interact with the protein or nucleic acid substrate. A similar binding mode was postulated for compound 20i within the active site of RNase H where the chelating triad in HID interacts with both the metal cofactors (Mn²⁺), while the CH₂ and C–H groups at the C4 and C5 position of compound 20i respectively interacts with the small hydrophobic residue A538 at the beginning of the pocket close to H539. The biaryl linker extends from the C6 position into the pocket lined up with hydrophobic residues W535 of the p66 subunit and W266, F346, and W426 of the p51 subunit. The predicted binding mode of both the compounds (7 and 20i) appears to satisfy the typically required chelating triad interaction with both the metal cofactors and the biaryl linker extends into the hydrophobic pocket (Figure 3, right), hence corroborating the active site inhibition mechanism against RNase H. As for polymerase binding, the uncompromised biochemical inhibition against NNRTI-resistant RT mutants strongly indicates that the NNRTI binding pocket is not occupied, consistent with our inability to stably dock our HID analogues into the NNRTI-binding pocket (data not shown). The exact binding mode for inhibition of RT polymerase activity is still unclear.

CONCLUSIONS

New HID chemotypes featuring a C-6 benzyl or biarylmethyl moiety were designed and synthesized as inhibitors of HIV RT associated RNase H domain. Key to the synthesis was the adaptation of a metal-free reductive benzylation and the masking of the requisite dicarboxylic acid. Primary biochemical assays with WT and NNRTI-resistant HIV RT showed that all

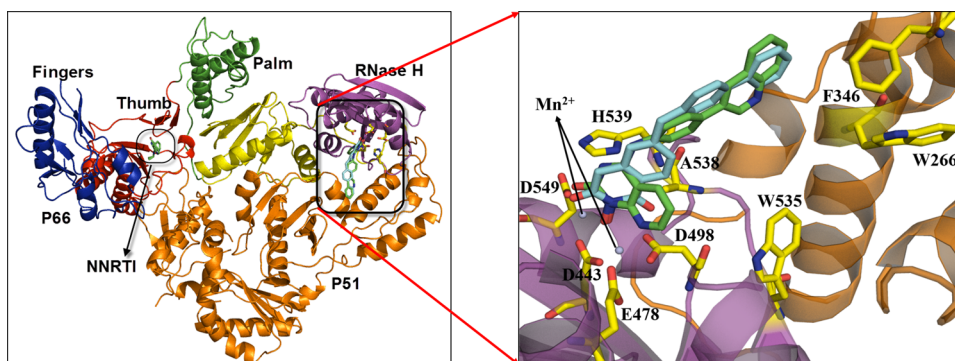


Figure 3. Binding mode of compound 20i. Left: structure of full length RT with two subunits p66 and p51 (orange). p66 subunit comprises fingers (blue), palm (red), thumb (green), connection (yellow), and RNase H (magenta) domains. Compounds 7 (green) and 20i (cyan) are docked into the RNase H active site. Right: a close-up view of RNase H active site with predicted binding mode of compound 7 (green) and 20i (cyan). Metal cofactors (Mn²⁺) are colored in gray, with the active site residues (D443, E478, D498 and D549) in yellow. Pictures were generated using PyMol.⁴¹

analogues of our new chemotypes were dually active against RNase H and polymerase in sub- to low-micromolar range. Additional testing demonstrated that our compounds also inhibit *E. coli* RNase H, as well as the polymerase, but not the RNase H, of MoMLV RT. Some analogues were also found active against HIV IN in a strand transfer assay, although the vast majority of the newly synthesized compounds, particularly the 6-biarylmethyl series, demonstrated a discernible preference toward RNase H and polymerase inhibition. Importantly, many of these new analogues inhibited HIV-1 in cell culture at low micromolar concentrations. Although the polymerase inhibition mechanism is not clear, molecular docking corroborates a mechanism of active site binding for RNase H inhibition. Collectively these studies established our new C6 benzyl and biarylmethyl scaffolds as potent dual inhibitors of HIV RT RNase H and polymerase, and that the additional polymerase inhibition may benefit active site RNase H inhibitors in achieving antiviral activity.

EXPERIMENTAL SECTION

Chemistry: General Procedures. All commercial chemicals were used as supplied unless otherwise indicated. Dry solvents were either purchased (toluene and dioxane) or dispensed under argon from an anhydrous solvent system with two packed columns of neutral alumina or molecular sieves (THF and DMF). Flash chromatography was performed on a Teledyne Combiflash RF-200 with RediSep columns (silica) and indicated mobile phase. All moisture sensitive reactions were performed under an inert atmosphere of ultrapure argon with oven-dried glassware. ^1H and ^{13}C NMR spectra were recorded on a Varian 600 MHz spectrometer. Mass data were acquired on an Agilent TOF II TOS/MS spectrometer capable of ESI and APCI ion sources. Analysis of sample purity was performed on a Varian Prepstar SD-1 HPLC system with a Phenomenex Gemini, 5 μm C18 column (250 mm \times 4.6 mm). HPLC conditions: solvent A = H_2O , solvent B = MeCN; flow rate = 1.0 mL/min; compounds were eluted with a gradient of 5% MeCN/ H_2O to 100% MeCN for 25 min. Purity was determined by total absorbance at 254 nm. All tested compounds have a purity $\geq 96\%$.

General Procedure 1 for the One-Pot Reductive Coupling of Aldehydes with Boronic Acids (14a–g). To a solution of aldehyde **12** (17.4 mmol, 1.0 equiv) in toluene (15 mL) was added TsNHNH_2 (1.34 g, 7.4 mmol, 1.0 equiv) and stirred at 80 $^\circ\text{C}$ for 2–3 h. The reaction was monitored by TLC. After complete consumption of aldehyde, solvent was removed under vacuo. Tosylhydrazone was further dried under high vacuum for several hours and used in the next step without further purification. To a solution of tosylhydrazone in dioxane (20 mL) was added potassium carbonate (1.02 g, 11.1 mmol, 1.5 equiv) and boronic acid (11.1 mmol, 1.5 equiv). The reaction mixture was refluxed for 2–4 h and monitored by TLC. The solvent was removed under reduced pressure, and saturated solution of NaHCO_3 was added and extracted with DCM (3 \times 50 mL). The combined organic layers were dried over Na_2SO_4 , filtered, and concentrated. The crude product was purified by flash column chromatography (EtOAc/hexane, 1:6) to afford desired compound (**14a–g**) as a solid.

5-Benzyl-2,3-dihydro-1H-inden-1-ol (14a). Yield 54%. ^1H NMR (CDCl_3 , 600 MHz) δ 7.32–7.26 (m, 4H), 7.22–7.20 (m, 2H), 7.09–7.08 (m, 2H), 5.22 (t, J = 6.6 Hz, 1H), 3.98 (s, 2H), 3.04–2.99 (m, 1H), 2.80–2.75 (m, 1H), 2.50–2.45 (m, 1H), 1.97–1.94 (m, 1H), 1.61 (s, 1H, OH).

General Procedure 2 for the Synthesis of Alkene (15a–g). To a solution of alcohol (3.45 mmol, 1.0 equiv) in toluene (20 mL) was added PPTS (10.37 mmol, 3.0 equiv). The reaction mixture was refluxed for 6–10 h and monitored by TLC and cooled to room temperature. The saturated NaHCO_3 solution was added, and the aqueous layer was extracted with EtOAc (3 \times 25 mL). The combined organic layers were dried over Na_2SO_4 , filtered, and concentrated. The crude product was purified by flash column chromatography (EtOAc/hexane, 1:99) to afford desired alkene (**15a–g**) as a solid.

6-Benzyl-1H-indene (15a). Yield 90%. ^1H NMR (CDCl_3 , 600 MHz) δ 7.23–7.17 (m, 4H), 7.14–7.12 (m, 3H), 7.03 (d, J = 7.8 Hz, 1H), 6.76–6.75 (m, 1H), 6.40–6.39 (m, 1H), 3.93 (s, 2H), 3.25 (s, 2H).

General Procedure 3 for the Synthesis of Diol (16a–g). To a solution of alkene (2.81 mmol, 1.0 equiv) in (acetone/*t*-butanol/water; 3:3:4; 20 mL) was added osmium tetroxide (2.5% solution in *t*-BuOH, 0.28 mmol, 0.1 equiv) and *N*-methylmorpholineoxide (4.22 mmol, 1.5 equiv) and stirred at room temperature for 4–10 h, and the reaction was monitored by TLC. After complete consumption of the starting material, sodium sulfite (4 equiv) was added and stirred at room temperature for 1 h more. The solvent was evaporated, and the aqueous layer was extracted with EtOAc (3 \times 25 mL). The combined organic layers were dried over Na_2SO_4 , filtered, and concentrated. The crude product was purified by flash column chromatography (EtOAc/hexane; 1.5:3.5) to afford desired diol (**16a–g**) as a solid.

5-Benzyl-2,3-dihydro-1H-indene-1,2-diol (16a). Yield 81%. ^1H NMR (CDCl_3 , 600 MHz) δ 7.34 (d, J = 7.8 Hz, 1H), 7.29–7.26 (m, 3H), 7.21–7.17 (m, 2H), 7.11 (d, J = 7.8 Hz, 1H), 7.06 (s, 1H), 4.97 (d, J = 4.8 Hz, 1H), 4.50–4.48 (m, 1H), 3.96 (s, 2H), 3.08 (dd, J = 6.0 Hz, J = 16.2 Hz, 1H), 2.90 (dd, J = 4.2 Hz, J = 16.2 Hz, 1H), 2.27 (s, 2H, 2-OH).

General Procedure 4 for the Synthesis of Dicarboxylic Acid (17a–g). The suspension of diol (1.86 mmol, 1.0 equiv) in $\text{CH}_3\text{CN}/\text{CCl}_4/\text{H}_2\text{O}$ (2:2:3; 20 mL) was sonicated to make a clear solution. After the addition of NaIO_4 (11.2 mmol, 6.0 equiv), the reaction mixture was stirred for 10 min, then treated with $\text{RuCl}_3 \cdot \text{H}_2\text{O}$ (0.19 mmol, 0.1 equiv). The reaction mixture was stirred for 30–40 min and monitored by TLC. The mixture was diluted with water and extracted with CH_2Cl_2 (3 \times 25 mL), and the combined organic layers were dried over Na_2SO_4 , filtered, and concentrated to give a black residue, then Et_2O was added to the residue and filtered through a short pad of Celite. The filtrate was concentrated to provide a brown oil and was triturated with ether to get dicarboxylic acid (**17a–g**) as a solid.

4-Benzyl-2-(carboxymethyl)benzoic Acid (17a). Yield 81%. ^1H NMR (CD_3OD , 600 MHz) δ 7.93 (d, J = 8.4 Hz, 1H), 7.27–7.25 (m, 2H), 7.21–7.18 (s, 4H), 7.15 (s, 1H), 4.00 (s, 2H), 3.96 (s, 2H).

General Procedure 5 for Suzuki Coupling (18h–t). The mixture of diacid **17e** (150 mg, 0.43 mmol), boronic acid (0.86 mmol, 2.0 equiv), K_2CO_3 (1.7 mmol, 4.0 equiv), $\text{EtOH}/\text{H}_2\text{O}$ (1:1, 4.0 mL), and $\text{Pd}[\text{P}(\text{Ph})_3]_4$ (30 mg) were microwaved at 120 $^\circ\text{C}$ for 20–30 min. The reaction was monitored by TLC and MS. The black residue formed was filtered, and the filtrate was concentrated under reduced pressure to remove EtOH. The aqueous mixture was washed with Et_2O and then acidified to pH 3. The white precipitate was obtained via filtration, dried under high vacuum overnight, and used in the next step without further purification.

4-([1,1'-Biphenyl]-4-ylmethyl)-2-(carboxymethyl)benzoic Acid (18i). Yield 75%. ^1H NMR (DMSO, 600 MHz) δ 7.83 (d, J = 7.8 Hz, 1H), 7.61 (d, J = 7.2 Hz, 2H), 7.57 (d, J = 8.4 Hz, 2H), 7.42 (t, J = 7.8 Hz, 2H), 7.33–7.31 (m, 3H), 7.25–7.23 (m, 2H), 3.99 (s, 2H), 3.88 (s, 2H).

General Procedure 6 for Cyclization and Deprotection (20a–t). A solution of dicarboxylic acid (0.28 mmol, 1.0 equiv) and NH_2OTHP (0.34 mmol, 1.2 equiv) in toluene (15 mL) was refluxed for 5 min. To the mixture, a solution of CDI in DCM (0.28 mmol, 1.0 equiv) was added dropwise. The suspension turned clear and stirred at reflux for 12 h, a black solid separated from solution, and the reaction monitored by TLC and MS. The reaction mixture was passed through a short pad of silica gel which then rinsed with (EtOAc/hexane, 1:3), the combined filtrate was evaporated to dryness. The product was used for the next reaction without further purification. The cyclized product was dissolved in MeOH (5.0 mL) and treated with pTSA hydrate (1.0 equiv) and stirred at room temperature for 2–3 h. Upon the disappearance of starting material by TLC, the mixture was evaporated to dryness to get pale-yellow solid. The solid obtained was triturated with water and then with ether and dried at room temperature to afford a desired pure compound (**20a–t**) as a solid.

6-Benzyl-2-hydroxyisoquinoline-1,3(2H,4H)-dione (20a). Yield 55% (for two steps from 17a). ¹H NMR (CD₃OD, 600 MHz) δ 8.02 (d, J = 8.4 Hz, 1H), 7.32 (d, J = 7.8 Hz, 1H), 7.28–7.25 (m, 2H), 7.22–7.18 (m, 4H), 4.84 (s, 2H), 4.03 (s, 2H). ¹³C NMR (CD₃OD, 150 MHz) δ 167.1, 162.2, 148.2, 139.9, 134.4, 128.6, 128.2, 128.1, 128.0, 127.5, 126.0, 122.8, 47.2, 41.2. HRMS-ESI(–) *m/z* calcd for C₁₆H₁₂NO₃, 266.0817 [M – H][–]; found, 266.0808.

2-Hydroxy-6-(4-methylbenzyl)isoquinoline-1,3(2H,4H)-dione (20b). Yield 54% (for two steps from 17b). ¹H NMR (CD₃OD, 600 MHz) δ 8.02 (d, J = 8.4 Hz, 1H), 7.30–7.29 (m, 1H), 7.20 (s, 1H), 7.09–7.08 (m, 4H), 4.15 (s, 2H), 3.98 (s, 2H), 2.27 (s, 3H). ¹³C NMR (CD₃OD, 150 MHz) δ 167.1, 162.2, 148.5, 136.8, 135.7, 134.3, 128.8, 128.5, 128.1, 127.4, 122.8, 40.8, 19.6. HRMS-ESI(–) *m/z* calcd for C₁₇H₁₄NO₃, 280.0974 [M – H][–]; found, 280.0961.

6-(4-Fluorobenzyl)-2-hydroxyisoquinoline-1,3(2H,4H)-dione (20c). Yield 51% (for two steps from 17c). ¹H NMR (DMSO, 600 MHz) δ 10.31 (s, 1H, OH), 7.92 (d, J = 7.8 Hz, 1H), 7.32 (d, J = 8.4 Hz, 1H), 7.28–7.26 (m, 2H), 7.23 (s, 1H), 7.10 (t, J = 9.0 Hz, 2H), 4.19 (s, 2H), 3.99 (s, 2H). ¹³C NMR (DMSO, 150 MHz) δ 166.7, 162.0, 147.6, 135.4, 131.1, 128.5, 128.3, 128.0, 123.6, 115.8, 115.6, 47.5, 37.3. HRMS-ESI(–) *m/z* calcd for C₁₆H₁₁NFO₃, 284.0723 [M – H][–]; found, 284.0722.

6-(4-Chlorobenzyl)-2-hydroxyisoquinoline-1,3(2H,4H)-dione (20d). Yield 51% (for two steps from 17d). ¹H NMR (CD₃OD, 600 MHz) δ 8.03 (d, J = 8.4 Hz, 1H), 7.31 (d, J = 3.9 Hz, 1H), 7.27–7.26 (m, 2H), 7.21–7.18 (m, 3H), 4.84 (s, 2H), 4.02 (s, 2H). ¹³C NMR (CD₃OD, 150 MHz) δ 167.1, 162.1, 147.6, 138.7, 134.5, 131.9, 130.2, 128.3, 128.2, 127.9, 127.5, 123.0, 48.1, 40.4. HRMS-ESI(–) *m/z* calcd for C₁₆H₁₁ClNO₃, 300.0427 [M – H][–]; found, 300.0420.

6-(4-Bromobenzyl)-2-hydroxyisoquinoline-1,3(2H,4H)-dione (20e). Yield 48% (for two steps from 17e). ¹H NMR (CD₃OD, 600 MHz) δ 7.95 (d, J = 7.8 Hz, 1H), 7.32–7.33 (m, 2H), 7.34–7.22 (m, 1H), 7.13 (s, 1H), 7.05 (d, J = 7.8 Hz, 2H), 4.75 (s, 2H), 3.92 (s, 2H). ¹H NMR (DMSO, 600 MHz) δ 10.39 (s, 1H, OH), 8.01 (d, J = 7.8 Hz, 1H), 7.55 (d, J = 7.8 Hz, 2H), 7.40 (d, J = 8.4 Hz, 1H), 7.30–7.27 (m, 3H), 4.27 (s, 2H), 4.06 (s, 2H). ¹³C NMR (CD₃OD, 150 MHz) δ 167.4, 162.2, 147.5, 139.3, 134.5, 131.3, 130.5, 128.3, 128.3, 127.9, 127.5, 125.5, 123.0, 119.8, 48.1, 40.4. HRMS-ESI(–) *m/z* calcd for C₁₆H₁₁BrNO₃, 343.9922 [M – H][–]; found, 343.9911.

2-Hydroxy-6-(4-(trifluoromethyl)benzyl)isoquinoline-1,3(2H,4H)-dione (20f). Yield 49% (for two steps from 17f). ¹H NMR (CD₃OD, 600 MHz) δ 8.06 (d, J = 8.4 Hz, 1H), 7.58 (d, J = 7.8 Hz, 2H), 7.42 (d, J = 7.8 Hz, 2H), 7.35 (d, J = 7.8 Hz, 1H), 7.25 (s, 1H), 4.84 (s, 2H), 4.14 (s, 2H). ¹³C NMR (CD₃OD, 150 MHz) δ 162.1, 147.0, 144.6, 134.6, 129.2, 128.3, 128.0, 127.6, 125.1, 123.2, 47.1, 40.4. HRMS-ESI(–) *m/z* calcd for C₁₇H₁₁F₃NO₃, 334.0691 [M – H][–]; found, 334.0679.

6-(2,4-Difluorobenzyl)-2-hydroxyisoquinoline-1,3(2H,4H)-dione (20g). Yield 50% (for two steps from 17g). ¹H NMR (CD₃OD, 600 MHz) δ 8.04 (d, J = 7.2 Hz, 1H), 7.32–7.28 (m, 2H), 7.22 (s, 1H), 6.97–6.89 (m, 2H), 4.17 (s, 2H), 4.04 (s, 2H). ¹³C NMR (CD₃OD, 150 MHz) δ 162.1, 146.5, 134.5, 131.8, 131.7, 128.2, 127.7, 127.3, 123.1, 111.0, 110.9, 103.4, 103.2, 103.0, 33.6. HRMS-ESI(–) *m/z* calcd for C₁₆H₁₀F₂NO₃, 302.0629 [M – H][–]; found, 302.0616.

6-(4-Cyclopropylbenzyl)-2-hydroxyisoquinoline-1,3(2H,4H)-dione (20h). Yield 54% (for two steps from 18h). ¹H NMR (CDCl₃, 600 MHz) δ 8.11 (d, J = 8.4 Hz, 1H), 7.24 (d, J = 8.4 Hz, 1H), 7.09 (s, 1H), 7.05 (d, J = 8.4 Hz, 2H), 7.02 (d, J = 8.4 Hz, 2H), 4.12 (s, 2H), 3.99 (s, 2H), 1.88–1.85 (m, 1H), 0.96–0.93 (m, 2H), 0.68–0.65 (m, 2H). HRMS-ESI(–) *m/z* calcd for C₁₉H₁₆NO₃, 306.1130 [M – H][–]; found, 306.1115.

6-([1,1'-Biphenyl]-4-ylmethyl)-2-hydroxyisoquinoline-1,3(2H,4H)-dione (20i). Yield 47% (for two steps from 18i). ¹H NMR (CDCl₃, 600 MHz) δ 8.15 (d, J = 7.8 Hz, 1H), 7.57–7.54 (m, 4H), 7.43 (t, J = 7.8 Hz, 2H), 7.38–7.34 (m, 2H), 7.24 (d, J = 7.8 Hz, 2H), 7.15 (s, 1H), 4.14 (s, 2H), 4.09 (s, 2H). ¹³C NMR (CDCl₃, 150 MHz) δ 163.5, 160.1, 148.4, 140.6, 139.7, 138.2, 133.3, 129.3, 129.2, 129.0, 128.8, 127.8, 127.5, 127.3, 126.9, 122.0, 41.5, 36.4. HRMS-ESI(–) *m/z* calcd for C₂₂H₁₆NO₃, 342.1130 [M – H][–]; found, 342.1111.

2-Hydroxy-6-(4-(thiophen-2-yl)benzyl)isoquinoline-1,3(2H,4H)-dione (20j). Yield 47% (for two steps from 18j). ¹H NMR (CDCl₃,

600 MHz) δ 8.14 (d, J = 7.2 Hz, 1H), 7.56 (d, J = 7.8 Hz, 2H), 7.35 (d, J = 8.4 Hz, 1H), 7.29–7.28 (m, 2H), 7.18 (d, J = 7.2 Hz, 2H), 7.12 (s, 1H), 7.07–7.06 (m, 1H), 4.14 (s, 2H), 4.05 (s, 2H). ¹³C NMR (CDCl₃, 150 MHz) δ 163.5, 160.2, 148.2, 143.8, 138.4, 133.3, 129.4, 129.2, 128.9, 128.0, 127.8, 126.3, 124.8, 123.1, 122.0, 44.6, 41.5, 36.4. HRMS-ESI(–) *m/z* calcd for C₂₀H₁₄NSO₃, 348.0694 [M – H][–]; found, 348.0677.

6-((4'-Fluoro-[1,1'-biphenyl]-4-yl)methyl)-2-hydroxyisoquinoline-1,3(2H,4H)-dione (20k). Yield 45% (for two steps from 18k). ¹H NMR (CDCl₃/DMSO, 600 MHz) δ 8.20 (d, J = 7.2 Hz, 1H), 7.62–7.58 (m, 5H), 7.45 (d, J = 6.6 Hz, 1H), 7.35 (d, J = 6.6 Hz, 2H), 7.21–7.19 (m, 2H), 4.23 (s, 2H), 4.17 (s, 2H). ¹³C NMR (CDCl₃/DMSO, 150 MHz) δ 162.1, 161.5, 148.0, 138.5, 136.8, 133.6, 132.7, 131.7, 129.3, 128.9, 128.6, 128.3, 127.8, 127.6, 122.9, 115.4, 115.2, 41.2, 36.7. HRMS-ESI(–) *m/z* calcd for C₂₂H₁₅FNO₃, 360.1036 [M – H][–]; found, 360.1023.

4'-((2-Hydroxy-1,3-dioxo-1,2,3,4-tetrahydroisoquinolin-6-yl)methyl)-[1,1'-biphenyl]-4-carbonitrile (20l). Yield 37% (for two steps from 18l). ¹H NMR (DMSO, 600 MHz) δ 10.28 (br s, 1H), 7.95 (d, J = 8.4 Hz, 1H), 7.89 (d, J = 8.4 Hz, 2H), 7.84 (d, J = 8.4 Hz, 2H), 7.67 (d, J = 7.2 Hz, 2H), 7.39–7.36 (m, 3H), 7.28 (s, 1H), 4.21 (s, 2H), 4.06 (s, 2H). ¹³C NMR (DMSO, 150 MHz) δ 166.7, 162.0, 147.4, 144.8, 141.5, 136.7, 135.4, 133.3, 130.0, 128.5, 128.4, 128.1, 127.8, 123.6, 119.3, 110.3, 40.9, 37.4. HRMS-ESI(–) *m/z* calcd for C₂₃H₁₅N₂O₃, 367.1083 [M – H][–]; found, 367.1068.

2-Hydroxy-6-((4'-methoxy-[1,1'-biphenyl]-4-yl)methyl)isoquinoline-1,3(2H,4H)-dione (20m). Yield 41% (for two steps from 18m). ¹H NMR (CDCl₃/DMSO, 600 MHz) δ 8.14 (d, J = 6.6 Hz, 1H), 7.50–7.48 (m, 4H), 7.37 (d, J = 6.6 Hz, 1H), 7.21 (d, J = 7.2 Hz, 2H), 7.14 (s, 1H), 6.79 (d, J = 8.4 Hz, 2H), 4.13 (s, 2H), 4.07 (s, 2H), 3.84 (s, 3H). ¹³C NMR (CDCl₃/DMSO, 150 MHz) δ 166.4, 161.9, 159.1, 148.2, 139.2, 137.8, 133.5, 133.3, 129.3, 129.1, 128.8, 128.0, 127.7, 127.0, 122.9, 114.2, 55.3, 49.4, 41.5. HRMS-ESI(–) *m/z* calcd for C₂₃H₁₈NO₄, 372.1236 [M – H][–]; found, 372.1223.

2-Hydroxy-6-((4'-(methylsulfonyl)-[1,1'-biphenyl]-4-yl)methyl)isoquinoline-1,3(2H,4H)-dione (20n). Yield 48% (for two steps from 18n). ¹H NMR (CDCl₃, 600 MHz) δ 8.16 (d, J = 8.4 Hz, 1H), 8.00 (d, J = 7.8 Hz, 2H), 7.75 (d, J = 9.0 Hz, 2H), 7.56 (d, J = 8.4 Hz, 2H), 7.37 (d, J = 8.4 Hz, 1H), 7.29 (d, J = 8.4 Hz, 2H), 7.15 (s, 1H), 4.15 (s, 2H), 4.11 (s, 2H), 3.09 (s, 3H). ¹³C NMR (CDCl₃, 150 MHz) δ 163.4, 159.9, 147.8, 146.0, 139.9, 139.2, 137.6, 133.4, 129.7, 129.3, 128.9, 127.9, 127.8, 122.2, 44.6, 41.5, 36.4. HRMS-ESI(–) *m/z* calcd for C₂₃H₁₈NSO₄, 420.0906 [M – H][–]; found, 420.0891.

4'-((2-Hydroxy-1,3-dioxo-1,2,3,4-tetrahydroisoquinolin-6-yl)methyl)-[1,1'-biphenyl]-4-sulfonamide (20o). Yield 36% (for two steps from 18o). ¹H NMR (DMSO, 600 MHz) δ 10.21 (br s, 1H), 7.95 (d, J = 7.8 Hz, 1H), 7.85 (d, J = 7.8 Hz, 2H), 7.81 (d, J = 7.8 Hz, 2H), 7.65 (d, J = 8.4 Hz, 2H), 7.38–7.36 (m, 4H), 4.21 (s, 2H), 4.06 (s, 2H). ¹³C NMR (DMSO, 150 MHz) δ 166.7, 162.0, 147.5, 143.5, 143.2, 141.0, 137.1, 135.2, 130.0, 128.5, 128.4, 128.1, 127.7, 127.4, 126.7, 123.6, 40.9, 37.4. HRMS-ESI(–) *m/z* calcd for C₂₂H₁₇N₂SO₃, 421.0858 [M – H][–]; found, 421.0851.

4'-((2-Hydroxy-1,3-dioxo-1,2,3,4-tetrahydroisoquinolin-6-yl)methyl)-[1,1'-biphenyl]-4-carboxamide (20p). Yield 35% (for two steps from 18p). ¹H NMR (DMSO, 600 MHz) δ 7.95 (d, J = 7.8 Hz, 1H), 7.92 (d, J = 8.4 Hz, 2H), 7.71 (d, J = 7.8 Hz, 2H), 7.65 (d, J = 8.4 Hz, 2H), 7.38–7.35 (m, 3H), 7.29 (s, 1H), 4.21 (s, 2H), 4.05 (s, 2H). ¹³C NMR (DMSO, 150 MHz) δ 167.9, 166.7, 162.0, 147.5, 142.8, 140.6, 137.7, 135.4, 133.4, 129.9, 128.5, 128.4, 128.1, 127.6, 127.5, 126.7, 125.9, 123.6, 40.9, 37.3. HRMS-ESI(–) *m/z* calcd for C₂₃H₁₇N₂O₄, 385.1188 [M – H][–]; found, 385.1173.

6-((2',4'-Difluoro-[1,1'-biphenyl]-4-yl)methyl)-2-hydroxyisoquinoline-1,3(2H,4H)-dione (20q). Yield 42% (for two steps from 18q). ¹H NMR (CDCl₃, 600 MHz) δ 8.08 (d, J = 7.8 Hz, 1H), 7.38 (d, J = 8.4 Hz, 2H), 7.31–7.29 (m, 2H), 7.17 (d, J = 7.8 Hz, 2H), 7.08 (s, 1H), 6.88–6.82 (m, 2H), 4.08 (s, 2H), 4.02 (s, 2H). ¹³C NMR (CDCl₃, 150 MHz) δ 163.5, 160.0, 148.1, 138.7, 133.4, 133.3, 131.3, 129.3, 129.2, 129.0, 127.8, 126.7, 122.1, 111.7, 111.5, 104.4, 41.6, 36.4. HRMS-ESI(–) *m/z* calcd for C₂₂H₁₄F₂NO₃, 378.0942 [M – H][–]; found, 378.0929.

6-((2',4'-Bis(trifluoromethyl)-[1,1'-biphenyl]-4-yl)methyl)-2-hydroxyisoquinoline-1,3(2H,4H)-dione (**20r**). Yield 39% (for two steps from **18r**). ¹H NMR (CDCl₃, 600 MHz) δ 8.10 (d, *J* = 7.8 Hz, 1H), 7.93 (s, 1H), 7.75 (d, *J* = 8.4 Hz, 1H), 7.40 (d, *J* = 7.8 Hz, 1H), 7.31 (d, *J* = 7.8 Hz, 1H), 7.20 (d, *J* = 8.4 Hz, 2H), 7.16 (d, *J* = 8.4 Hz, 2H), 7.09 (s, 1H), 4.10 (s, 2H), 4.05 (s, 2H). ¹³C NMR (CDCl₃, 150 MHz) δ 163.5, 160.0, 147.9, 144.6, 139.4, 136.8, 133.4, 132.8, 129.9, 129.2, 129.1, 129.0, 128.6, 128.5, 128.2, 128.1, 127.9, 123.4, 122.2, 41.6, 36.4. HRMS-ESI(-) *m/z* calcd for C₂₄H₁₄F₆NO₃, 478.0878 [M - H]⁻; found, 478.0874.

6-((3'-Fluoro-4'-methoxy-[1,1'-biphenyl]-4-yl)methyl)-2-hydroxyisoquinoline-1,3(2H,4H)-dione (**20s**). Yield 41% (for two steps from **18s**). ¹H NMR (CDCl₃, 600 MHz) δ 8.14 (d, *J* = 7.2 Hz, 1H), 7.48 (d, *J* = 7.2 Hz, 2H), 7.36 (d, *J* = 7.2 Hz, 1H), 7.31–7.26 (m, 3H), 7.22 (d, *J* = 7.2 Hz, 2H), 7.01 (t, *J* = 8.4 Hz, 1H), 4.14 (s, 2H), 4.07 (s, 2H), 3.92 (s, 3H). ¹³C NMR (CDCl₃, 150 MHz) δ 160.2, 153.4, 148.3, 138.2, 133.8, 133.3, 129.4, 129.2, 128.9, 127.8, 127.1, 122.5, 120.0, 114.7, 113.7, 56.4, 41.5, 36.4. HRMS-ESI(-) *m/z* calcd for C₂₃H₁₇FNO₄, 390.1142 [M - H]⁻; found, 390.1130.

4-(4-((2-Hydroxy-1,3-dioxo-1,2,3,4-tetrahydroisoquinolin-6-yl)methyl)phenyl)pyridin-1-ium 4-methylbenzenesulfonate (**20t**). Yield 49% (for two steps from **18t**). ¹H NMR (CDCl₃, 600 MHz) δ 8.92 (d, *J* = 6.0 Hz, 2H), 8.37 (d, *J* = 6.0 Hz, 2H), 7.98–7.94 (m, 3H), 7.52 (d, *J* = 7.8 Hz, 2H), 7.46 (d, *J* = 7.8 Hz, 2H), 7.39 (d, *J* = 8.4 Hz, 1H), 7.30 (s, 1H), 7.09 (d, *J* = 7.8 Hz, 2H), 4.20 (s, 2H), 4.13 (s, 2H), 2.26 (s, 3H). ¹³C NMR (CDCl₃, 150 MHz) δ 166.7, 162.0, 155.7, 146.9, 146.2, 144.9, 142.8, 138.0, 135.4, 132.7, 130.5, 128.8, 128.6, 128.5, 128.4, 128.2, 125.9, 123.9, 123.7, 40.9, 37.4, 21.2. HRMS-ESI(-) *m/z* calcd for C₂₁H₁₅N₂O₃, 343.1083 [M - H]⁻; found, 343.1070.

Biology. Reagents. Biologicals. Recombinant HIV-1 reverse transcriptase (RT) was expressed and purified as previously described.⁴² The catalytically active RNase H domain fragment of HIV-1 RT was expressed from plasmid pCSR231 (a generous gift from Dr. Daria Hazuda, Merck, West Point, PA) and purified as previously described.⁴³ P4R5 HIV infection indicator cells were obtained from the NIH AIDS Reagent Program, Division of AIDS, NIAID, NIH (p4R5.MAGI from Dr. Nathaniel Landau). These cells express CD4, CXCR4, and CCR5 as well as a β-galactosidase reporter gene under the control of an HIV LTR promoter.

The *Escherichia coli* RNase H plasmid pSM101 was obtained from Dr. Susan Marqusee (University of California Berkeley) and *E. coli* RNase H was expressed and purified as previously described.⁴⁴ Recombinant Moloney Murine Leukemia Virus (MoMLV) reverse transcriptase (RT) was expressed and purified as previously described.⁴⁵

Chemicals. DNA and RNA oligonucleotides for the preparation of RNA/DNA duplexes for assay of RNase H activity were purchased from Trilink (San Diego, CA).

RNase H Assay. RNase H activity was measured essentially as previously described.³² Three different RNA/DNA duplex substrates were used, each assessing a different mode of RNase H cleavage. HTS-1 (RNA 5'-gaucugagccggagcu-3'-fluorescein annealed to DNA 3'-CTAGACTCGGACCCTCGA-5'-Dabcyl) is a high sensitivity duplex that assesses nonspecific internal cleavage. HTS-2 (RNA 5'-cugguagaccagaucugagccggagcu-3'-fluorescein annealed to DNA 3'-GGTCTAGACTCGGACCCTCGA-5'-Dabcyl) provides a duplex with a recessed DNA 3'-terminus and measures 3'-DNA directed or polymerase directed RNase H cleavage. HTS-3 (RNA 5'-accagaucugagccggagcu-3'-fluorescein annealed to DNA 3'-GACCAATCTGGTCTAGACTCGGACCCTCGA-5'-Dabcyl) measures 5'-RNA-directed RNase H cleavage.

For *E. coli* RNase H assays, 4 nM of enzyme was incubated with 6 mM MgCl₂ and 1, 7, or 30 μM inhibitor (final concentration of DMSO was 2%) in 50 mM Tris pH 7.8, 50 mM NaCl for 10 min at room temperature before initiation of the reaction by addition of 100 nM HTS-1 RNA/DNA substrate. Reactions were carried out at 37 °C and were stopped after 5 min by the addition of EDTA at a final concentration of 33 mM. For MoMLV RT RNase H assays, 20 nM enzyme was incubated with 1 mM MnCl₂ and 1, 7, or 30 μM inhibitor

(final concentration of DMSO was 2%) in 50 mM Tris pH 7.8, 60 mM KCl, 0.1 mg/mL BSA, 0.01% NP-40, and 1 mM DTT for 10 min at room temperature before initiation of the reaction by addition of 100 nM HTS-1 RNA/DNA substrate. Reactions were carried out at 37 °C and were stopped after 15 min by the addition of EDTA at a final concentration of 33 mM. Fluorescence signals were measured 485/528 nm excitation/emission wavelengths in an EnSpire multimode plate reader (PerkinElmer, Waltham, MA). The results were plotted using GraphPad Prism 5 (GraphPad Software, Inc., La Jolla, CA), and 50% inhibitory concentrations (IC₅₀s) were obtained at midpoint concentrations.⁴⁶ Duplicate reactions were performed in at least two independent experiments.

RT Polymerase Assay. HIV RT polymerase activity was determined in the presence and the absence of inhibitor using 10 μM [³H]-TTP and 40 nM poly(rA)-oligo(dT)₁₆ (both obtained from PerkinElmer, Waltham, MA) in 50 mM Tris-HCl, pH 7.4 (37 °C) containing 60 mM KCl and 5 mM MgCl₂. Reactions were initiated by the addition of 10 nM WT or mutant RT and carried out for 20 min at 37 °C. Reactions were quenched by 200 μL of ice-cold 10% TCA containing 20 mM sodium pyrophosphate and filtered using a 1.2 μm glass fiber filter 96-well plates (Millipore, Billerica, MA), followed by sequentially washing with 10% TCA and ethanol. The extent of radionucleotide incorporation was determined by liquid scintillation spectrometry.

For MoMLV RT polymerase assays, a 100 nt template DNA (5'-ATGTGTGTGCCCGTCTGTTGTGTGACTCTGGTAACTAGAGATCCCTCAGACCCCTTTAGTCAGTGTGGAATATCTCATAGCTTGGCGCCCGAACAGGGAC) was annealed in an equimolar amount to an 18 nt DNA primer (5'-GTCCTGTTCGGGCGCCA) to yield a T_{d100}/P_{d18} DNA-DNA substrate as previously described.⁴⁷ Reactions containing 20 nM MoMLV RT, 40 nM T_{d100}/P_{d18} DNA/DNA substrate, 50 μM dNTPs, 0.5 mM EDTA, 1 mM MnCl₂, and 1, 7, or 30 μM inhibitor (final concentration of DMSO was 2%) in 50 mM Tris pH 7.8, 60 mM KCl, 0.1 mg/mL BSA, 0.01% NP-40, and 1 mM DTT were incubated for 30 min at 37 °C. All reactions were quenched by the addition of 50 μL of 100 mM EDTA and 2× QuantiFluor dsDNA reagent (Promega, Madison, WI) to quantify the amount of dsDNA in solution. Fluorescence signals were measured 504/531 nm excitation/emission wavelengths in an EnSpire multimode plate reader. The results were plotted using GraphPad Prism 5, and 50% inhibitory concentrations (IC₅₀s) were obtained at midpoint concentrations.⁴⁶ Duplicate reactions were performed in at least two independent experiments.

HIV IN Assay. HIV integrase was expressed and purified as previously reported.⁴⁸ Inhibition assays were performed using a modified protocol of our reported method.⁴⁸ Briefly, 2.1 μL of compound suspended in DMSO was placed in duplicate into a Black 96-well nonbinding plate (Corning 3991). Compounds were plated in duplicate to a final concentration of 0.13–100 μM. To each well of the plate 186.9 μL of reaction mixture without DNA substrate was added (10 mM HEPES pH 7.5, 10% glycerol w/v, 10 mM MnCl₂, 1 mM DTT, 1 μM integrase). The enzyme was incubated with inhibitor for 10 min at 25 °C, after which the reaction was initiated by the addition of 21 μL of 500 nM oligo (5' biotin ATGTGGAAAATCTCTAGCA annealed with ACTGCTAGAGATTTCCACAT 3' Cys). Reactions were incubated at 37 °C for 30 min and then quenched by the addition of 5.2 μL of 500 mM EDTA. Each reaction was moved (200 μL) to a MultiScreen HTS PCR plate (Millipore MSSLBPC10) containing 20 μL of streptavidin agarose beads (Life Technologies S951) and incubated with shaking for 30 min. A vacuum manifold was used to remove the reaction mixture, and the beads were similarly washed 3 times with wash buffer (0.05% SDS, 1 mM EDTA in PBS). The plates were further washed 3 times with 200 μL of 50 mM NaOH to denature DNA not covalently linked to the biotin modification. For each denaturation step, the plate was incubated with shaking at 25 °C for 5 min, and the NaOH was removed by centrifugation at 1000g for 1 min. The reaction products were eluted from the beads by the addition of 150 μL of formamide. The plate was incubated at 25 °C for 10 min and read directly at 635/675 in a SpectraMax i3 plate reader (Molecular Devices).

Antiviral Assays. Antiviral assays were carried out using P4R5 indicator cells essentially as previously described.⁴⁹ P4R5 cells were cultured in 96-well microplates (5×10^3 cells per well and maintained in DMEM/10% FBS supplemented with puromycin ($0.5 \mu\text{g/mL}$)). Cells were incubated in the presence or the absence of drug for 16 h then exposed to HIV followed by an additional incubation period of 48 h. The extent of infection was assessed using a fluorescence-based β -galactosidase detection assay, as previously described.³⁷

Modeling and Docking. Molecular modeling was performed using the Schrodinger small molecule Drug Discovery Suite 2013-2. The crystal structure of full length RT cocrystallized with naphthyridinone-based scaffold MK2 (PDB code: 3LP1) was obtained from Protein Data Bank⁵⁰ as reported by Munsu et al.³⁹ The above RT structure was subjected to analysis and found that the native ligand MK2 was bound to the active site of RNase H, which is $\sim 50 \text{ \AA}$ from the NNRTI site. This model was subjected to Protein Preparation Wizard^{51,52} (Schrodinger Inc.) in which missing hydrogens atoms were added, zero-order bonds to metals were created followed by the generation of metal binding states. The structure of protein was minimized using OPLS 2005 force field⁵³ to optimize hydrogen bonding network and converge heavy atoms to the RMSD of 0.3 \AA . The processed model indicates that the interaction between the naphthyridinone and RNase H is mediated by two metals cations (Mn^{2+}) coordinated by the active site residues D443, E478, D498, and D549.

The receptor grid generation tool in Maestro (Schrodinger Inc.)⁵⁴ was used to define an active site around the MK2 ligand to cover all the residues within 12 \AA from it with both the metal cofactors (Mn^{2+}) as a constraint to identify the chelating triad during docking. The ligands compounds 7 and 20i were drawn using Maestro and subjected to Lig Prep⁵⁵ to generate conformers, possible protonation at pH of 7 ± 3 and metal binding states which serves as an input for docking process. All the dockings were performed using Glide XP⁴⁰ (Glide, version 6.0) mode with both the Mn^{2+} metal cofactors as a constraint. The van der Waals radii of nonpolar atoms for each of the ligands were scaled by a factor of 0.8. The predicted highly scored binding mode of both the compounds 7 and 20i features the critical interaction between the chelating triad to the divalent metal cofactors, suggesting a possible conformation. All the ligands within the active site of RNase H were further refined post docking by minimizing under implicit solvent to account for the local protein flexibility.

■ ASSOCIATED CONTENT

Supporting Information

Characterization data, including ^1H NMR, ^{13}C NMR, and HRMS data, of all intermediates. This material is available free of charge via the Internet at <http://pubs.acs.org>.

■ AUTHOR INFORMATION

Corresponding Author

*Phone: +1 (612) 626-7025. E-mail: wangx472@umn.edu.

Present Address

^{||}(For Z.L.) Key Laboratory of Pesticide & Chemical Biology, Ministry of Education, College of Chemistry, Central China Normal University, 152 Luoyu Road, Wuhan, Hubei 430079, China

Notes

The authors declare no competing financial interest.

■ ACKNOWLEDGMENTS

This research was supported in part by the National Institutes of Health (AI100890 to S.G.S., M.A.P., and Z.W.), and by the Research Development and Seed Grant Program of the Center for Drug Design, University of Minnesota.

■ ABBREVIATIONS USED

RT, reverse transcriptase; HIV, human immunodeficiency virus; RNase H, ribonuclease H; HID, 2-hydroxyisoquinoline-1,3-dione; IN, integrase; NRTIs, nucleoside RT inhibitors; NNRTIs, nonnucleoside RT inhibitors; WT, wild-type; DMF, *N,N*-dimethylformamide; PPTS, pyridinium *p*-toluenesulfonate; THP, tetrahydropyran; *p*-TSA, *p*-toluenesulfonic acid; SAR, structure–activity relationship; RISF, retroviral integrase superfamily; ST, strand transfer

■ REFERENCES

- (1) *AIDSinfo*; UNAIDS: Geneva 2013; <http://www.unaids.org/en/dataanalysis/datatools/aidsinfo/>.
- (2) Barouch, D. H. Challenges in the development of an HIV-1 vaccine. *Nature* **2008**, *455*, 613–619.
- (3) Schiffner, T.; Sattentau, Q. J.; Dorrell, L. Development of prophylactic vaccines against HIV-1. *Retrovirology* **2013**, *10*, 72.
- (4) Zhang, J.; Crumpacker, C. Eradication of HIV and Cure of AIDS, Now and How? *Front. Immunol.* **2013**, *4*, 337.
- (5) Siliciano, J. D.; Siliciano, R. F. HIV-1 eradication strategies: design and assessment. *Curr. Opin. HIV AIDS* **2013**, *8*, 318–325.
- (6) Xing, S.; Siliciano, R. F. Targeting HIV latency: pharmacologic strategies toward eradication. *Drug Discovery Today* **2013**, *18*, 541–551.
- (7) Beilartz, G. L.; Gotte, M. HIV-1 Ribonuclease H: Structure, Catalytic Mechanism and Inhibitors. *Viruses* **2010**, *2*, 900–926.
- (8) Sarafianos, S. G.; Marchand, B.; Das, K.; Himmel, D. M.; Parniak, M. A.; Hughes, S. H.; Arnold, E. Structure and function of HIV-1 reverse transcriptase: molecular mechanisms of polymerization and inhibition. *J. Mol. Biol.* **2009**, *385*, 693–713.
- (9) Cihlar, T.; Ray, A. S. Nucleoside and nucleotide HIV reverse transcriptase inhibitors: 25 years after zidovudine. *Antiviral Res.* **2010**, *85*, 39–58.
- (10) de Bethune, M. P. Non-nucleoside reverse transcriptase inhibitors (NNRTIs), their discovery, development, and use in the treatment of HIV-1 infection: a review of the last 20 years (1989–2009). *Antiviral Res.* **2010**, *85*, 75–90.
- (11) Corona, A.; Masaoka, T.; Tocco, G.; Tramontano, E.; Le Grice, S. F. Active site and allosteric inhibitors of the ribonuclease H activity of HIV reverse transcriptase. *Future Med. Chem.* **2013**, *5*, 2127–2139.
- (12) Ilna, T.; Labarge, K.; Sarafianos, S. G.; Ishima, R.; Parniak, M. A. Inhibitors of HIV-1 Reverse Transcriptase-Associated Ribonuclease H Activity. *Biology (Basel, Switzerland)* **2012**, *1*, 521–541.
- (13) Klumpp, K.; Hang, J. Q.; Rajendran, S.; Yang, Y. L.; Derosier, A.; In, P. W. K.; Overton, H.; Parkes, K. E. B.; Cammack, N.; Martin, J. A. Two-metal ion mechanism of RNA cleavage by HIV RNase H and mechanism-based design of selective HIV RNase H inhibitors. *Nucleic Acids Res.* **2003**, *31*, 6852–6859.
- (14) Himmel, D. M.; Sarafianos, S. G.; Dharmasena, S.; Hossain, M. M.; McCoy-Simandle, K.; Ilna, T.; Clark, A. D.; Knight, J. L.; Julius, J. G.; Clark, P. K.; Krogh-Jespersen, K.; Levy, R. M.; Hughes, S. H.; Parniak, M. A.; Arnold, E. HIV-1 reverse transcriptase structure with RNase H inhibitor dihydroxy benzoyl naphthyl hydrazone bound at a novel site. *ACS Chem. Biol.* **2006**, *1*, 702–712.
- (15) Fuji, H.; Urano, E.; Futahashi, Y.; Hamatake, M.; Tatsumi, J.; Hoshino, T.; Morikawa, Y.; Yamamoto, N.; Komano, J. Derivatives of 5-nitro-furan-2-carboxylic acid carbamoylmethyl ester inhibit RNase H activity associated with HIV-1 reverse transcriptase. *J. Med. Chem.* **2009**, *52*, 1380–1387.
- (16) Tramontano, E.; Esposito, F.; Badas, R.; Di Santo, R.; Costi, R.; La Colla, P. 6-[1-(4-Fluorophenyl)methyl-1H-pyrrol-2-yl]-2,4-dioxo-5-hexenoic acid ethyl ester a novel diketo acid derivative which selectively inhibits the HIV-1 viral replication in cell culture and the ribonuclease H activity in vitro. *Antiviral Res.* **2005**, *65*, 117–124.
- (17) Lansdon, E. B.; Liu, Q.; Leavitt, S. A.; Balakrishnan, M.; Perry, J. K.; Lancaster-Moyer, C.; Kutty, N.; Liu, X.; Squires, N. H.; Watkins, W. J.; Kirschberg, T. A. Structural and binding analysis of pyrimidinol

carboxylic acid and *N*-hydroxy quinazolinedione HIV-1 RNase H inhibitors. *Antimicrob. Agents Chemother.* **2011**, *55*, 2905–2915.

(18) Williams, P. D.; Staas, D. D.; Venkatraman, S.; Loughran, H. M.; Ruzek, R. D.; Booth, T. M.; Lyle, T. A.; Wai, J. S.; Vacca, J. P.; Feuston, B. P.; Ecto, L. T.; Flynn, J. A.; DiStefano, D. J.; Hazuda, D. J.; Bahnck, C. M.; Himmelberger, A. L.; Dornadula, G.; Hrin, R. C.; Stillmock, K. A.; Witmer, M. V.; Miller, M. D.; Grobler, J. A. Potent and selective HIV-1 ribonuclease H inhibitors based on a 1-hydroxy-1,8-naphthyridin-2(1*H*)-one scaffold. *Bioorg. Med. Chem. Lett.* **2010**, *20*, 6754–6757.

(19) Gerondelis, P.; Johns, B. A., The development of novel pyridopyrimidinone antiretrovirals with selective activity against HIV ribonuclease H. , Cold Spring Harbor Laboratories Conference on Retroviruses, Cold Spring Harbor, NY, May 21–26, 2012; Cold Spring Harbor Press: Cold Spring Harbor, NY, 2012.

(20) Beilhartz, G. L.; Ngure, M.; Johns, B. A.; DeAnda, F.; Gerondelis, P.; Gotte, M. Inhibition of the Ribonuclease H Activity of HIV-1 Reverse Transcriptase by GSK5750 Correlates with Slow Enzyme–Inhibitor Dissociation. *J. Biol. Chem.* **2014**, *289*, 16270–16277.

(21) Chen, Y. L.; Tang, J.; Kesler, M. J.; Sham, Y. Y.; Vince, R.; Geraghty, R. J.; Wang, Z. Q. The design, synthesis and biological evaluations of C-6 or C-7 substituted 2-hydroxyisoquinoline-1,3-diones as inhibitors of hepatitis C virus. *Bioorg. Med. Chem.* **2012**, *20*, 467–479.

(22) Billamboz, M.; Bailly, F.; Lion, C.; Calmels, C.; Andreola, M. L.; Witvrouw, M.; Christ, F.; Debyser, Z.; De Luca, L.; Chimirri, A.; Cotelte, P. 2-Hydroxyisoquinoline-1,3(2*H*,4*H*)-diones as inhibitors of HIV-1 integrase and reverse transcriptase RNase H domain: influence of the alkylation of position 4. *Eur. J. Med. Chem.* **2011**, *46*, 535–546.

(23) Billamboz, M.; Suchaud, V.; Bailly, F.; Lion, C.; Demeulemeester, J.; Calmels, C.; Andreola, M. L.; Christ, F.; Debyser, Z.; Cotelte, P. 4-Substituted 2-Hydroxyisoquinoline-1,3-(2*H*,4*H*)-diones as a Novel Class of HIV-1 Integrase Inhibitors. *ACS Med. Chem. Lett.* **2013**, *4*, 41–46.

(24) Desimmie, B. A.; Demeulemeester, J.; Suchaud, V.; Taltynov, O.; Billamboz, M.; Lion, C.; Bailly, F.; Strelkov, S. V.; Debyser, Z.; Cotelte, P.; Christ, F. 2-Hydroxyisoquinoline-1,3(2*H*,4*H*)-diones (HIDs), Novel Inhibitors of HIV Integrase with a High Barrier to Resistance. *ACS Chem. Biol.* **2013**, *8*, 1187–1194.

(25) Suchaud, V.; Bailly, F.; Lion, C.; Calmels, C.; Andréola, M.-L.; Christ, F.; Debyser, Z.; Cotelte, P. Investigation of a Novel Series of 2-Hydroxyisoquinoline-1,3(2*H*,4*H*)-diones as Human Immunodeficiency Virus Type 1 Integrase Inhibitors. *J. Med. Chem.* **2014**, *57*, 4640–4660 <http://dx.doi.org/10.1021/jm500109z>.

(26) Billamboz, M.; Bailly, F.; Lion, C.; Touati, N.; Vezin, H.; Calmels, C.; Andreola, M. L.; Christ, F.; Debyser, Z.; Cotelte, P. Magnesium Chelating 2-Hydroxyisoquinoline-1,3(2*H*,4*H*)-diones, as Inhibitors of HIV-1 Integrase and/or the HIV-1 Reverse Transcriptase Ribonuclease H Domain: Discovery of a Novel Selective Inhibitor of the Ribonuclease H Function. *J. Med. Chem.* **2011**, *54*, 1812–1824.

(27) Billamboz, M.; Bailly, F.; Barreca, M. L.; De Luca, L.; Mouscadet, J. F.; Calmels, C.; Andreola, M. L.; Witvrouw, M.; Christ, F.; Debyser, Z.; Cotelte, P. Design, Synthesis, and Biological Evaluation of a Series of 2-Hydroxyisoquinoline-1,3(2*H*,4*H*)-diones as Dual Inhibitors of Human Immunodeficiency Virus Type 1 Integrase and the Reverse Transcriptase RNase H Domain. *J. Med. Chem.* **2008**, *51*, 7717–7730.

(28) Barluenga, J.; Tomas-Gamasa, M.; Aznar, F.; Valdes, C. Metal-free carbon–carbon bond-forming reductive coupling between boronic acids and tosylhydrazones. *Nature Chem.* **2009**, *1*, 494–499.

(29) Vanrheenen, V.; Cha, D. Y.; Hartley, W. M. Catalytic Osmium-Tetroxide Oxidation of Olefins—*cis*-1,2-Cyclohexanediol. *Org. Synth.* **1988**, *50*–9, 342–348.

(30) Vanrheenen, V.; Kelly, R. C.; Cha, D. Y. Improved Catalytic OsO₄ Oxidation of Olefins to *cis*-1,2-Glycols Using Tertiary Amine Oxides as Oxidant. *Tetrahedron Lett.* **1976**, 1973–1976.

(31) Yang, D.; Zhang, C. Ruthenium-catalyzed oxidative cleavage of olefins to aldehydes. *J. Org. Chem.* **2001**, *66*, 4814–4818.

(32) Parniak, M. A.; Min, K. L.; Budihis, S. R.; Le Grice, S. F.; Beutler, J. A. A fluorescence-based high-throughput screening assay for inhibitors of human immunodeficiency virus-1 reverse transcriptase-associated ribonuclease H activity. *Anal. Biochem.* **2003**, *322*, 33–39.

(33) Parniak, M. A.; Min, K. L. Substrate for assaying ribonuclease H activity. US 7,186,520 March 6, 2007.

(34) Parniak, M. A.; Min, K. L. Method of identifying or characterizing a compound that modulates ribonuclease H activity. US 7,439,035 October 21, 2008.

(35) Nowotny, M. Retroviral integrase superfamily: the structural perspective. *EMBO Rep.* **2009**, *10*, 144–151.

(36) Barreca, M. L.; Ferro, S.; Rao, A.; De Luca, L.; Zappala, M.; Monforte, A. M.; Debyser, Z.; Witvrouw, M.; Chimirri, A. Pharmacophore-based design of HIV-1 integrase strand-transfer inhibitors. *J. Med. Chem.* **2005**, *48*, 7084–7088.

(37) Abram, M. E.; Parniak, M. A. Virion instability of human immunodeficiency virus type 1 reverse transcriptase (RT) mutated in the protease cleavage site between RT p51 and the RT RNase H domain. *J. Virol.* **2005**, *79*, 11952–11961.

(38) Parikh, U. M.; Koontz, D. L.; Chu, C. K.; Schinazi, R. F.; Mellors, J. W. In vitro activity of structurally diverse nucleoside analogs against human immunodeficiency virus type 1 with the K65R mutation in reverse transcriptase. *Antimicrob. Agents Chemother.* **2005**, *49*, 1139–1144.

(39) Su, H.-P.; Yan, Y.; Prasad, G. S.; Smith, R. F.; Daniels, C. L.; Abeywickrema, P. D.; Reid, J. C.; Loughran, H. M.; Kornienko, M.; Sharma, S.; Grobler, J. A.; Xu, B.; Sardana, V.; Allison, T. J.; Williams, P. D.; Darke, P. L.; Hazuda, D. J.; Munshi, S. Structural Basis for the Inhibition of RNase H Activity of HIV-1 Reverse Transcriptase by RNase H Active Site-Directed Inhibitors. *J. Virol.* **2010**, *84*, 7625–7633.

(40) Friesner, R. A.; Murphy, R. B.; Repasky, M. P.; Frye, L. L.; Greenwood, J. R.; Halgren, T. A.; Sanschagrin, P. C.; Mainz, D. T. Extra precision glide: docking and scoring incorporating a model of hydrophobic enclosure for protein-ligand complexes. *J. Med. Chem.* **2006**, *49*, 6177–6196.

(41) PyMOL, *The PyMOL Molecular Graphics System*, version 1.5.0.4; Schrödinger, LLC: New York 2013.

(42) Fletcher, R. S.; Holleschak, G.; Nagy, E.; Arion, D.; Borkow, G.; Gu, Z.; Wainberg, M. A.; Parniak, M. A. Single-step purification of recombinant wild-type and mutant HIV-1 reverse transcriptase. *Protein Express. Purif.* **1996**, *7*, 27–32.

(43) Gong, Q.; Menon, L.; Ilina, T.; Miller, L. G.; Ahn, J.; Parniak, M. A.; Ishima, R. Interaction of HIV-1 reverse transcriptase ribonuclease H with an acylhydrazone inhibitor. *Chem. Biol. Drug Des.* **2011**, *77*, 39–47.

(44) Dabora, J. M.; Marqusee, S. Equilibrium unfolding of *Escherichia coli* ribonuclease H: characterization of a partially folded state. *Protein Sci.* **1994**, *3*, 1401–1408.

(45) Ndongwe, T. P.; Adedeji, A. O.; Michailidis, E.; Ong, Y. T.; Hachiya, A.; Marchand, B.; Ryan, E. M.; Rai, D. K.; Kirby, K. A.; Whately, A. S.; Burke, D. H.; Johnson, M.; Ding, S.; Zheng, Y. M.; Liu, S. L.; Kodama, E.; Delviks-Frankenberry, K. A.; Pathak, V. K.; Mitsuya, H.; Parniak, M. A.; Singh, K.; Sarafianos, S. G. Biochemical, inhibition and inhibitor resistance studies of xenotropic murine leukemia virus-related virus reverse transcriptase. *Nucleic Acids Res.* **2012**, *40*, 345–359.

(46) Kirby, K. A.; Marchand, B.; Ong, Y. T.; Ndongwe, T. P.; Hachiya, A.; Michailidis, E.; Leslie, M. D.; Sietsema, D. V.; Fetterly, T. L.; Dorst, C. A.; Singh, K.; Wang, Z.; Parniak, M. A.; Sarafianos, S. G. Structural and inhibition studies of the RNase H function of xenotropic murine leukemia virus-related virus reverse transcriptase. *Antimicrob. Agents Chemother.* **2012**, *56*, 2048–2061.

(47) Michailidis, E.; Marchand, B.; Kodama, E. N.; Singh, K.; Matsuoka, M.; Kirby, K. A.; Ryan, E. M.; Sawani, A. M.; Nagy, E.; Ashida, N.; Mitsuya, H.; Parniak, M. A.; Sarafianos, S. G. Mechanism of inhibition of HIV-1 reverse transcriptase by 4'-ethynyl-2'-fluoro-2'-deoxyadenosine triphosphate, a translocation-defective reverse transcriptase inhibitor. *J. Biol. Chem.* **2009**, *284*, 35681–35691.

(48) Wang, Z.; Bennett, E. M.; Wilson, D. J.; Salomon, C.; Vince, R. Rationally designed dual inhibitors of HIV reverse transcriptase and integrase. *J. Med. Chem.* **2007**, *50*, 3416–3419.

(49) Sirivolu, V. R.; Vernekar, S. K. V.; Iliina, T.; Myshakina, N. S.; Parniak, M. A.; Wang, Z. Q. Clicking 3'-Azidothymidine into Novel Potent Inhibitors of Human Immunodeficiency Virus. *J. Med. Chem.* **2013**, *56*, 8765–8780.

(50) *HIV-1 reverse transcriptase with inhibitor*; RCSB Protein Data Bank: Piscataway, NJ, 2010; <http://www.rcsb.org/pdb/explore.do?structureId=3LP1>, DOI: 10.2210/pdb3lp1/pdb .

(51) Sastry, G. M.; Adzhigirey, M.; Day, T.; Annabhimoju, R.; Sherman, W. Protein and ligand preparation: parameters, protocols, and influence on virtual screening enrichments. *J. Comput.-Aided Mol. Des.* **2013**, *27*, 221–234.

(52) (a) *Schrödinger Release 2013-2: Schrödinger Suite 2013 Protein Preparation Wizard*; Schrödinger, LLC: New York, 2013; (b) *Schrödinger Release 2013-2: Epik*, version 2.5; Schrödinger, LLC: New York, 2013; (c) *Schrödinger Release 2013-2: Impact*, version 6.0; Schrödinger, LLC: New York, 2013; (d) *Schrödinger Release 2013-2: Prime*, version 3; Schrödinger, LLC: New York, 2013.

(53) Jorgensen, W. L.; Maxwell, D. S.; TiradoRives, J. Development and testing of the OPLS all-atom force field on conformational energetics and properties of organic liquids. *J. Am. Chem. Soc.* **1996**, *118*, 11225–11236.

(54) *Schrödinger Release 2013-2: Maestro*, version 9.5; Schrödinger, LLC, New York, 2013.

(55) *Schrödinger Release 2013-2: LigPrep*, version 2.7; Schrödinger, LLC, New York, 2013.